ATLAS results on charmonium and B meson production and decays

Marcella Bona
(QMUL)
on behalf of the
ATLAS collaboration

41st International Conference on High Energy Physics
(ICHEP 2022)
Bologna, Italy
July 8th, 2022

b quarks in ATLAS

- 25 fb^{-1} in Run 1, and 139 fb^{-1} in Run 2
- Has access to all B hadrons
  - B, B_s, B_c, Λ_b, etc.
- Focus mostly on final states with muons
  - Typical trigger: di-muons with p_T thresholds at 4, 6 and 11 GeV
  - In 2018, a di-electron high-level trigger implemented and being analysed now

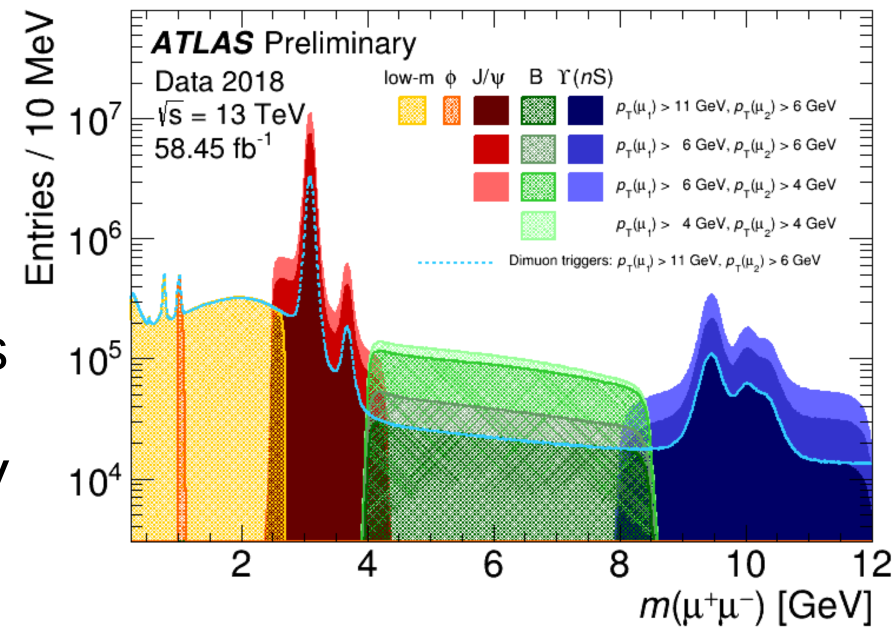

- **Properties of b-quark fragmentation to $B^\pm \rightarrow J/\psi K^\pm$ in Run 2**
  - arXiv:2108.11650, JHEP 12 (2021) 131
- **Measurement of relative B_c^+ /B^+ production in Run 1**
  - arXiv: 1912.02672, PRD 104 (2021) 012010
- **Production cross section of J/ψ and ψ(2S) at high p_T**
  - ATLAS-CONF-2019-047
- **Study of $B_c^+ \rightarrow J/\psi D_s$ decays in Run 2**
  - arXiv:2203.01808, CERN-EP-2022-025

Properties of b-quark fragmentation to $B^{\pm} \to J/\psi K^{\pm}$

Run-2 result:

arXiv:2108.11650, JHEP 12 (2021) 131

Properties of b-quark fragmentation

arXiv:2108.11650
JHEP 12 (2021) 131

- 139 fb^{-1} of Run-2 data
- b-fragmentation functions provide:
  - Test of QCD at LHC energy; MC tunes
  - $H \rightarrow b\bar{b}$ and many other channels with b-jet signatures - dominant uncertainty
- We measure longitudinal (z) and transverse (p_T^{rel}) projections of the $B^{\pm}$ momentum to jet axis.

$$z = \frac{\vec{p}_J \cdot \vec{p}_B}{\left|\vec{p}_J\right|^2}; \qquad p_T^{\mathrm{rel}} = \frac{\left|\vec{p}_J \times \vec{p}_B\right|}{\left|\vec{p}_J\right|}$$

- $B^{\pm}$ mesons are associated to jets if they are within $\Delta R = 0.4$ from jet axis.
- $B^{\pm}$ invariant mass is used to extract differential cross section in each z or p_T^{rel} bins, for jet momentum bins:
  50 GeV < p_T < 70 GeV,
  70 GeV < p_T < 100 GeV
  and p_T > 100 GeV.

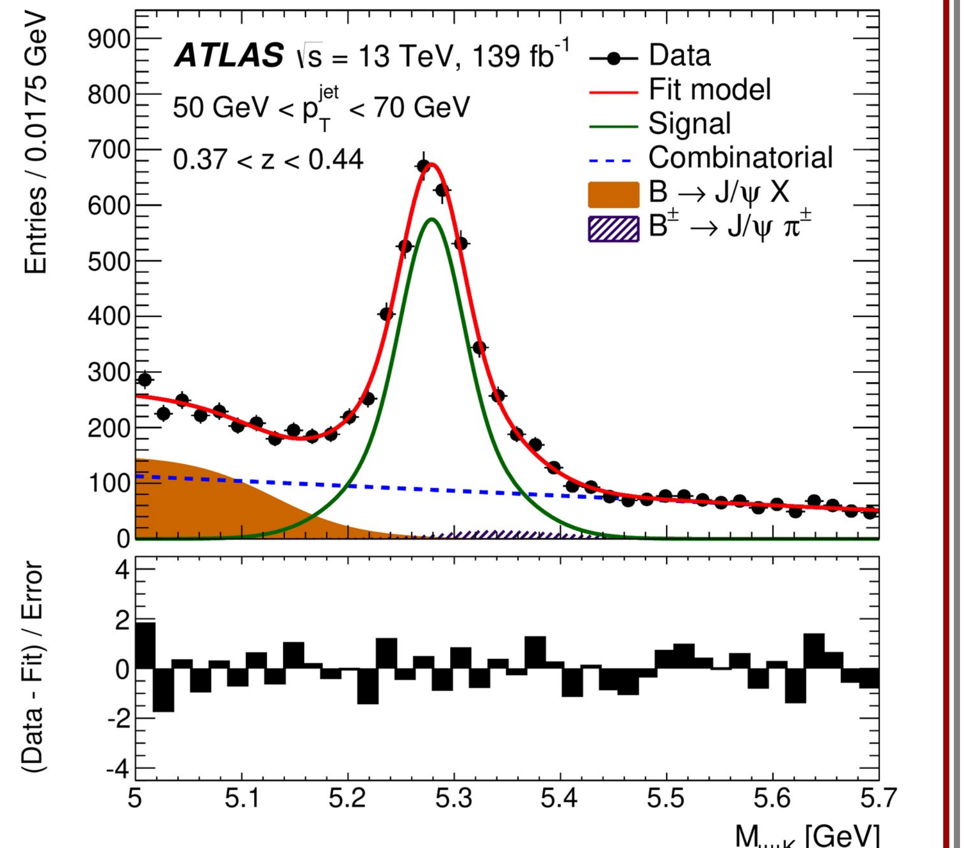

Properties of b-quark fragmentation

arXiv:2108.11650
JHEP 12 (2021) 131

- Results for z distributions for the lowest and highest jet p_T bins: 50 GeV < p_T < 70 GeV and p_T > 100 GeV

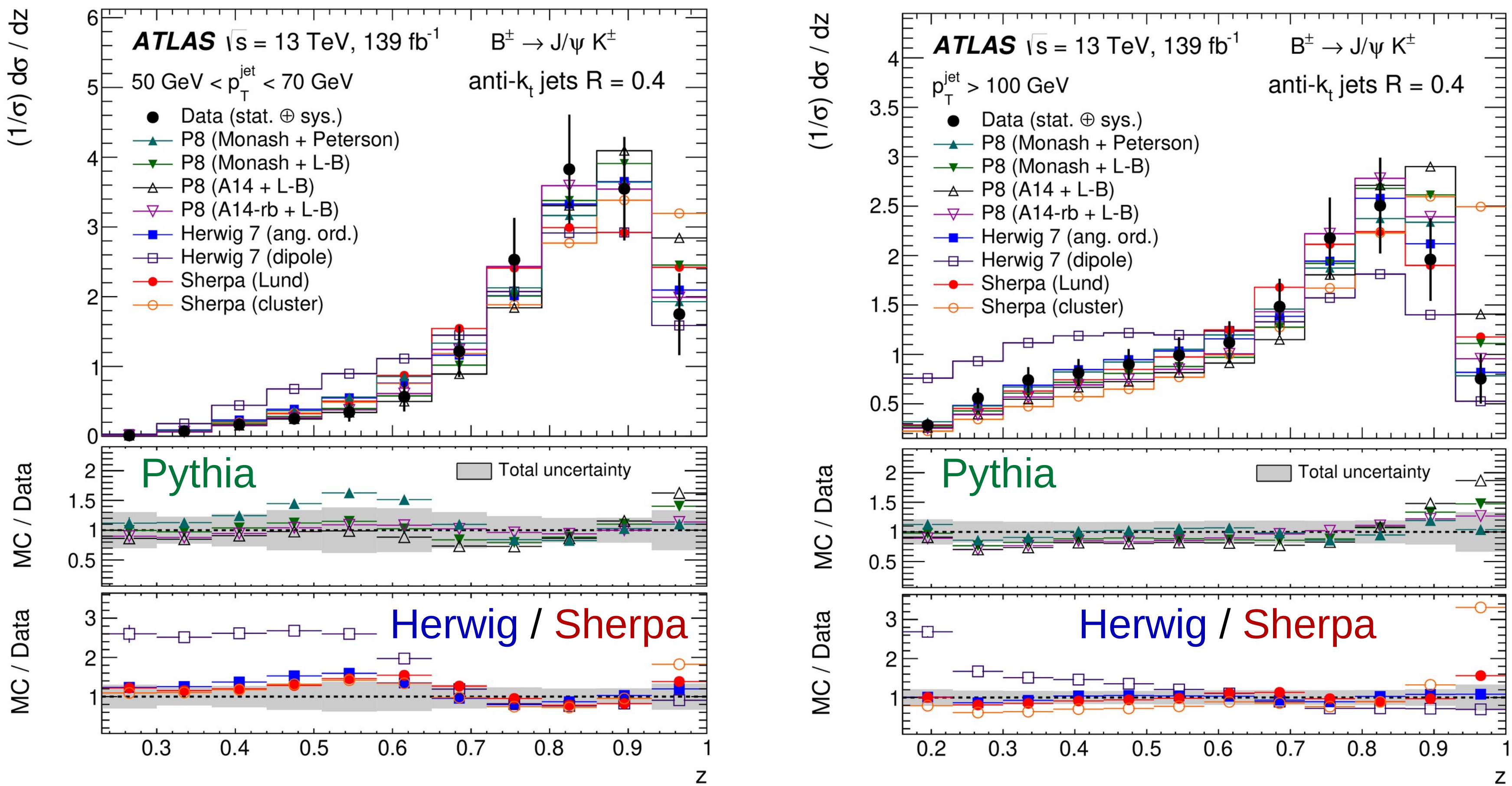

- lower tails of z distributions contain larger fraction of data at high p_T
  - gluon splitting has larger probability at higher p_T values → b quarks in the same jet and B meson from fragmentation of one b → leading to smaller values of z and higher values of p_T^{rel}

Properties of b-quark fragmentation

arXiv:2108.11650
JHEP 12 (2021) 131

- Results for z distributions for the lowest and highest jet p_T bins: 50 GeV < p_T < 70 GeV and p_T > 100 GeV

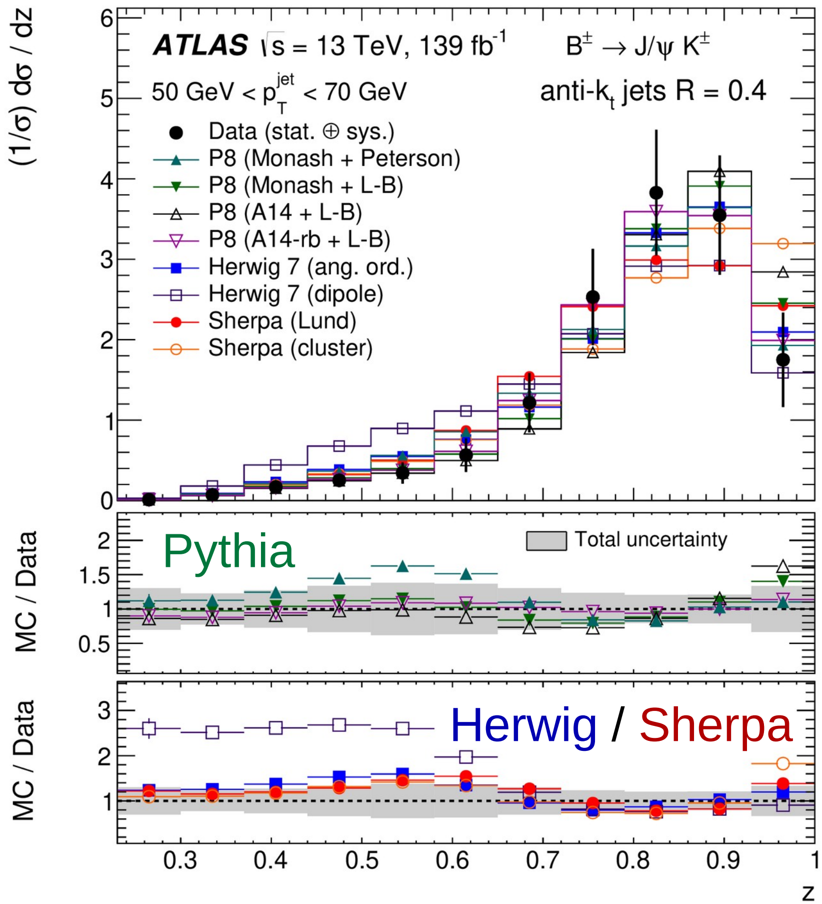

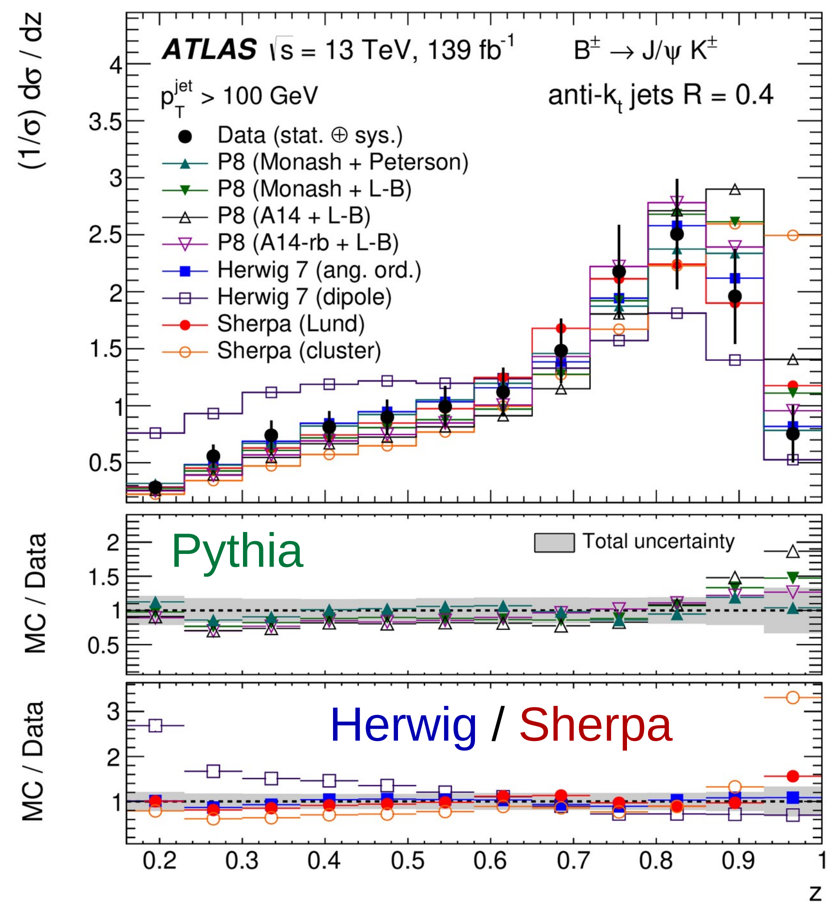

- All Pythia fragmentation models give a decent description.
- Herwig7 with dipole parton shower overestimates the low z tail at low p_T
  - larger fraction of jets arising from gluon splittings
- Sherpa (mainly cluster hadronisation model) differs for very high z

Properties of b-quark fragmentation

arXiv:2108.11650
JHEP 12 (2021) 131

- Results for p_T^{rel} distributions for the lowest and highest jet p_T bins:
  50 GeV < p_T < 70 GeV and p_T > 100 GeV

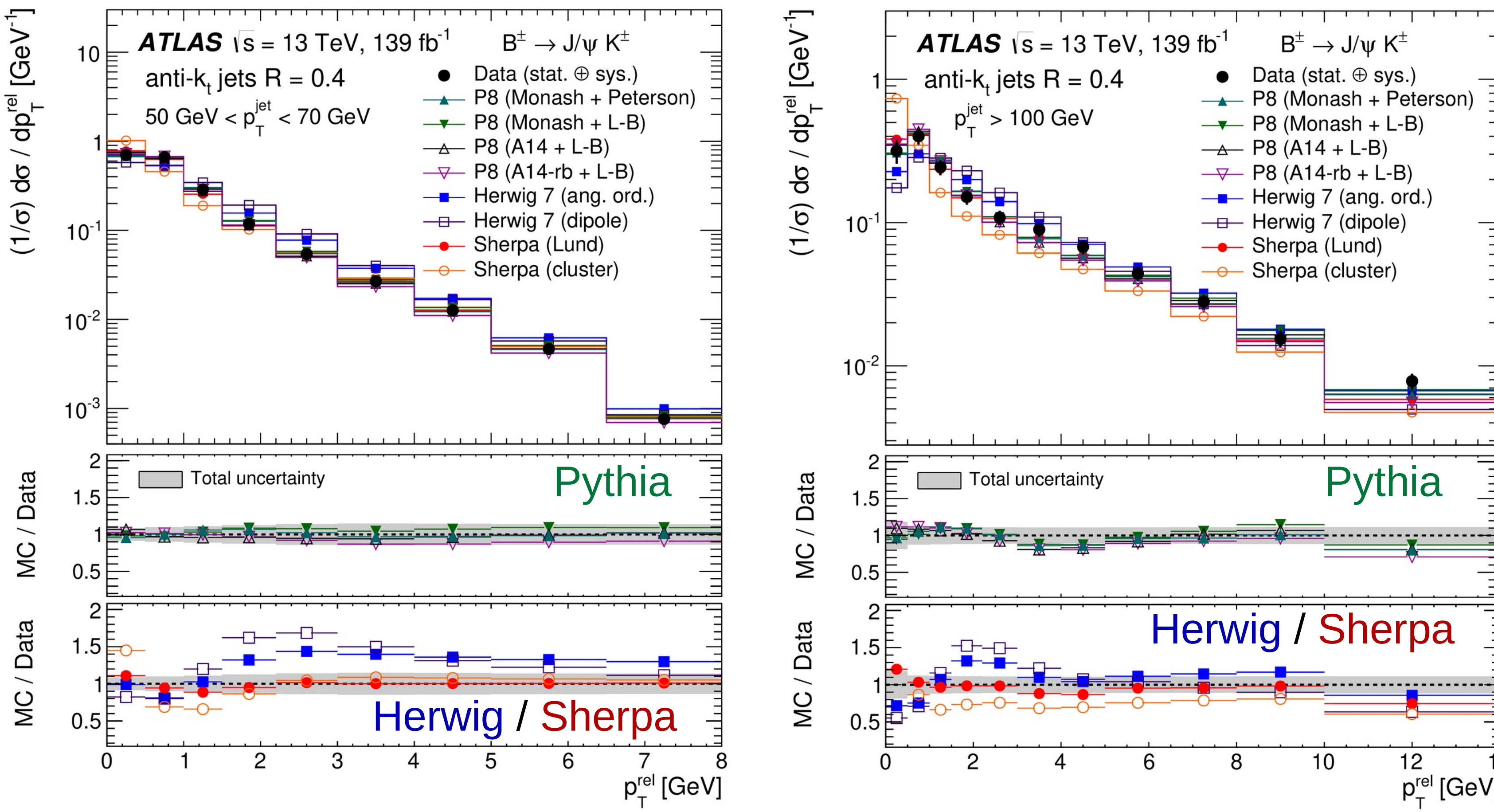

- All Pythia fragmentation models give a decent description.
- Herwig7 with dipole PS overestimates for p_T^{rel} in [1.5, 4.0] GeV at low p_T
- Sherpa (mainly cluster HM) discrepant for low values of p_T^{rel}, gets worse for higher jet p_T.

Properties of b-quark fragmentation

arXiv:2108.11650
JHEP 12 (2021) 131

- test of scale dependence: average values of the longitudinal profile <z> and of the transverse profile $\langle p_T^{rel} \rangle$ as a function of the jet p_T

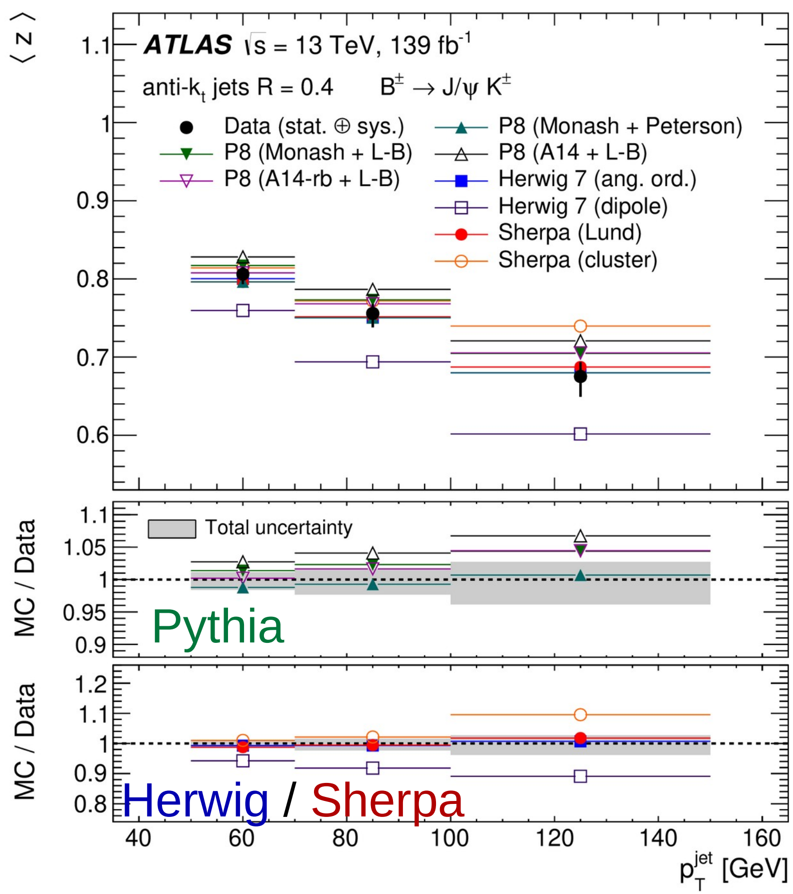

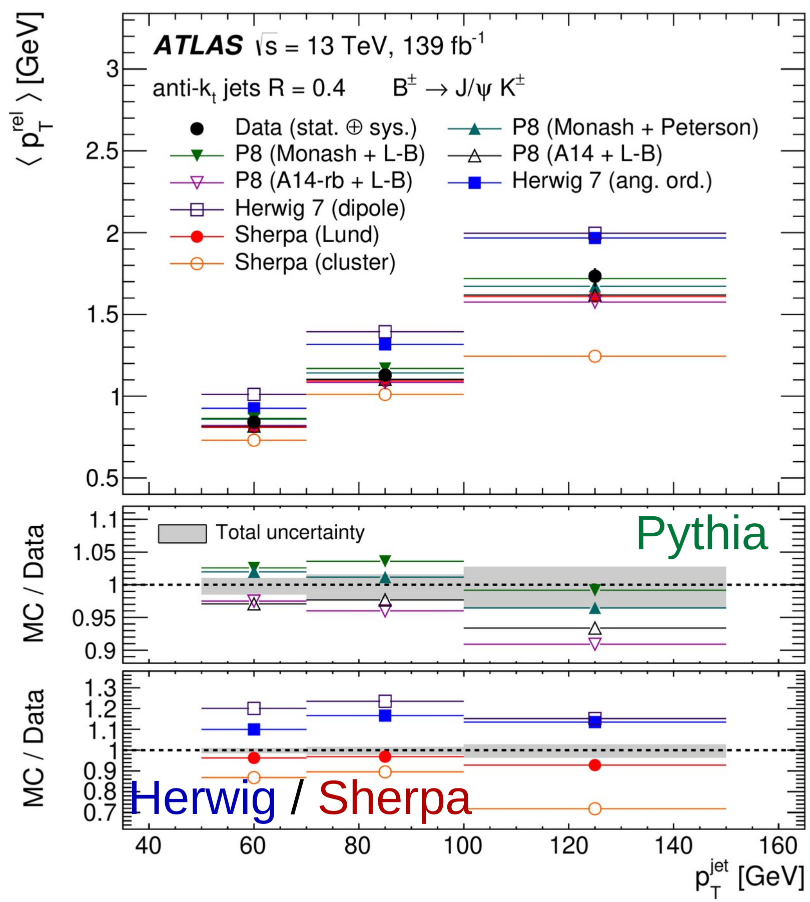

- Pythia (A14*) predicts slightly larger <z> and slightly lower $\langle p_T^{rel} \rangle$
- Both Herwig7 discrepant at 15-20% level in $\langle p_T^{rel} \rangle$ profile
- Sherpa (cluster) disagreeing at 10% to 25% for $\langle p_T^{rel} \rangle$

Relative B_c^+/B^+ production

Run-1 result:

arXiv: 1912.02672, PRD 104 (2021) 012010

Relative B_c^+/B^+ production

arXiv: 1912.02672,
PRD 104 (2021) 012010

- B_c^+ produced via collinear double-heavy quark production $b\bar{b}$ and $c\bar{c}$
  - unique insight into heavy-quark hadronisation
  - very wide ranges in theoretical predictions
- In Run-1 data at 8 TeV, we measure the ratio: $\dfrac{\sigma(B_c^\pm)\cdot\mathcal{B}(B_c^\pm\to J/\psi\pi^\pm)}{\sigma(B^\pm)\cdot\mathcal{B}(B^\pm\to J/\psi K^\pm)}$

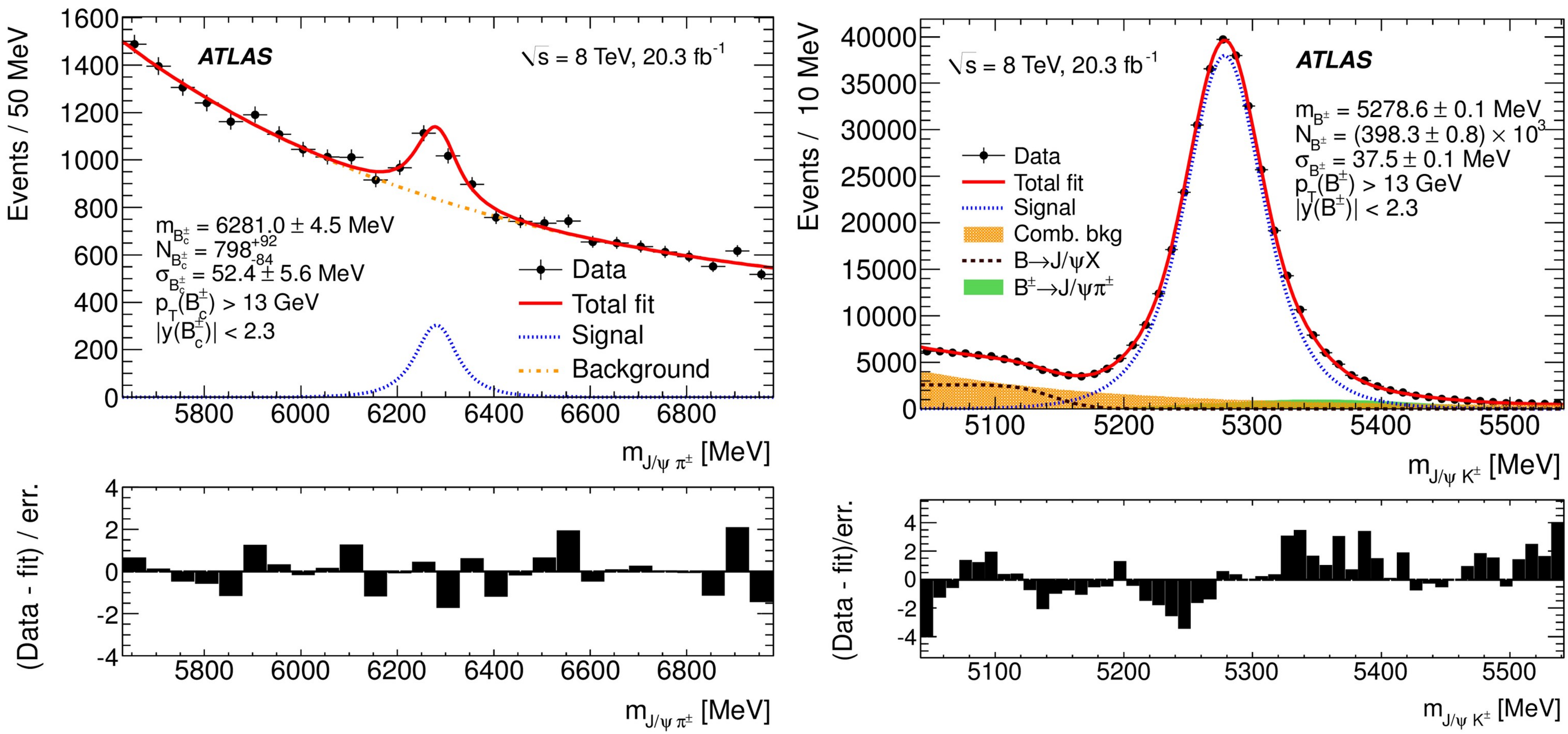

Relative B_c^+/B^+ production

arXiv: 1912.02672,
PRD 104 (2021) 012010

- Cross section ratio in entire fiducial volume $p_T(B) > 13$ GeV, $|y(B)| < 2.3$

$$\frac{\sigma(B_c^\pm)\cdot\mathcal{B}(B_c^\pm\to J/\psi\pi^\pm)}{\sigma(B^\pm)\cdot\mathcal{B}(B^\pm\to J/\psi K^\pm)} = (0.34 \pm 0.04(\text{stat.})^{+0.06}_{-0.02}(\text{syst.}) \pm 0.01\ (\text{lifetime}))\%$$

- Cross section ratio in bins of $p_T(B)$ and $|y(B)|$
  - With $p_T(B)$, the B_c^+ production decreases faster than B^+
  - No obvious dependence on $|y(B)|$

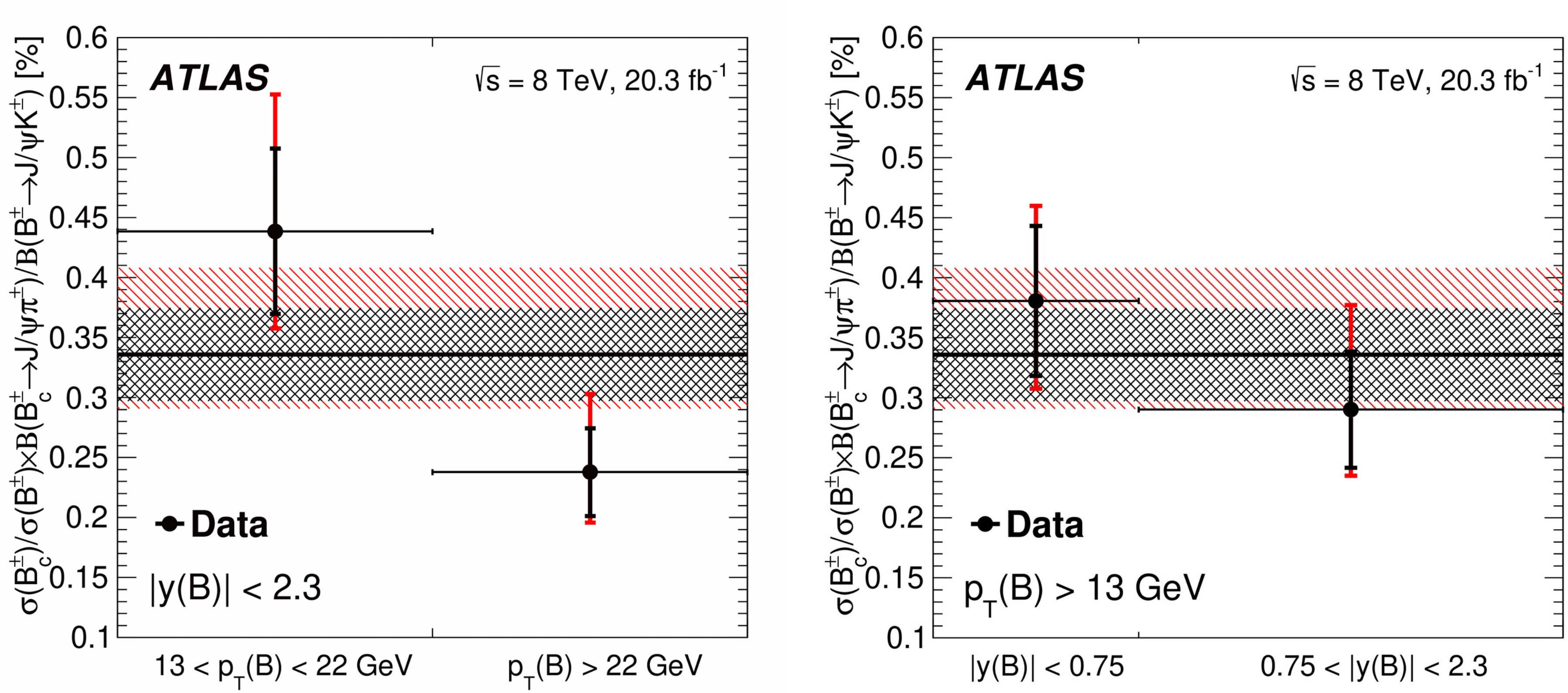

The points correspond to individual $p_T(B)$ or $|y(B)|$ bins. Shaded areas show result in the entire fiducial volume. Black - statistical uncertainties, red - statistical and systematic uncertainties.

Relative B_c^+/B^+ production

arXiv: 1912.02672,
PRD 104 (2021) 012010

- Cross section ratio in entire fiducial volume $p_T(B) > 13$ GeV, $|y(B)| < 2.3$

$$\frac{\sigma(B_c^\pm)\cdot\mathcal{B}(B_c^\pm\to J/\psi\pi^\pm)}{\sigma(B^\pm)\cdot\mathcal{B}(B^\pm\to J/\psi K^\pm)} = (0.34 \pm 0.04(\text{stat.})^{+0.06}_{-0.02}(\text{syst.}) \pm 0.01\ (\text{lifetime}))\%$$

- Cross section ratio in bins of $p_T(B)$ and $|y(B)|$
  - With $p_T(B)$, the B_c^+ production decreases faster than B^+
  - No obvious dependence on $|y(B)|$

Measurement	$p_T(B)$	$\|y(B)\|$	B_c^+/B^+ Ratio [%]
LHCb 8 TeV	< 20 GeV	$2.0-4.5$	$(0.683 \pm 0.018 \pm 0.009)$
CMS 7 TeV	> 15 GeV	< 1.6	$(0.48 \pm 0.05 \pm 0.03 \pm 0.05)$
ATLAS	$13-22$ GeV	< 2.3	$(0.44 \pm 0.07 \pm^{+0.09}_{-0.04} \pm 0.01)$
ATLAS	> 22 GeV	< 2.3	$(0.24 \pm 0.04 \pm^{+0.05}_{-0.01} \pm 0.01)$

LHCb: arXiv:1411.2943, Phys. Rev. Lett. 114, 132001 (2015)
CMS: arXiv:1410.5729, JHEP 01 (2015) 063

Production cross section of J/ψ and ψ(2S) at high p_T

Run-2 result:

ATLAS-CONF-2019-047

ATLAS-CONF-2019-047

Production cross section of J/ψ and ψ(2S)

- This analysis broadens the scope of comparison between experiment and theory by adding a high p_T selection on the quarkonium – this is expected to improve discrimination among competing models* of vector charmonium production.
- ATLAS has measured:
  - double differential production cross sections of J/ψ and ψ(2S) through their decays to $\mu^+\mu^-$.
  - prompt and non-prompt cross sections separately for both states.
  - for each state, the ratio of non-prompt to total (i.e. fraction of non-prompt).
  - for both prompt and non-prompt, the production ratios of ψ(2S) relative to J/ψ.
- Measured cross sections compared to predictions from FONLL model**, waiting for NRQCD predictions for high-p_T charmonium production.

* G. Li et al., PRD 83 (2011) 014001; J.P. Lansberg and C. Lorce, Phys. Lett. B 726 (2013) 218; B. Gong et al., JHEP 03 (2013) 115; M. Song et al., JHEP 02 (2011) 071; M. Butenschoen and B.A. Kniehl, Nucl. Phys. Proc. Suppl. 222-224 (2012) 151.
** FONLL (Fixed Order + Next-to-Leading Logarithms): M. Cacciari et al., JHEP 0103 (2001) 006; M. Cacciari et al., JHEP 1210 (2012) 137

ATLAS-CONF-2019-047

Production cross section of J/ψ and ψ(2S)

- Single muon trigger with threshold $p_T > 50$ GeV.
- J/ψ and ψ(2S) reconstructed via their decays to $\mu^+\mu^-$.
  - At least one muon must have $p_T > 52.5$ GeV.
- Sort data into (12 intervals in muon p_T) × (3 intervals in muon |y|).
- In each bin, extract yields N_{prompt} and $N_{non\text{-}prompt}$ from 2-dimensional unbinned max likelihood fit in dilepton mass m(μμ) and pseudo-proper decay time τ
- Compute double-differential cross section
  - A is acceptance, C is correction:

$$\frac{d^2\sigma^{\mathrm{P,NP}}(pp \to \psi)}{dp_T dy} \times \mathcal{B}(\psi \to \mu^+\mu^-) = \frac{1}{\mathcal{A}(\psi)} C_{\mathrm{BM}}\, C_{\mathrm{AP}} \frac{N_\psi^{\mathrm{P,NP}}}{\Delta p_T\, \Delta y \int \mathcal{L} dt}$$

- And non-prompt fractions and production ratios of ψ(2S) over J/ψ:

$$F_\psi^{\mathrm{NP}}(p_\mathrm{T}, y) = \frac{N_\psi^{\mathrm{NP}}}{N_\psi^{\mathrm{P}} + N_\psi^{\mathrm{NP}}}.$$

$$R^{\mathrm{P,NP}}(p_\mathrm{T}, y) = \left(\frac{\mathcal{A}(\psi(2\mathrm{S}))}{\mathcal{A}(J/\psi)}\right)^{-1} \frac{N_{\psi(2\mathrm{S})}^{\mathrm{P,NP}}}{N_{J/\psi}^{\mathrm{P,NP}}}$$

ATLAS-CONF-2019-047

Production cross section of J/ψ and ψ(2S)

- Example results:
  - Similar p_T dependence for prompt and non-prompt cross sections
  - Non-prompt fraction close to constant in this p_T range

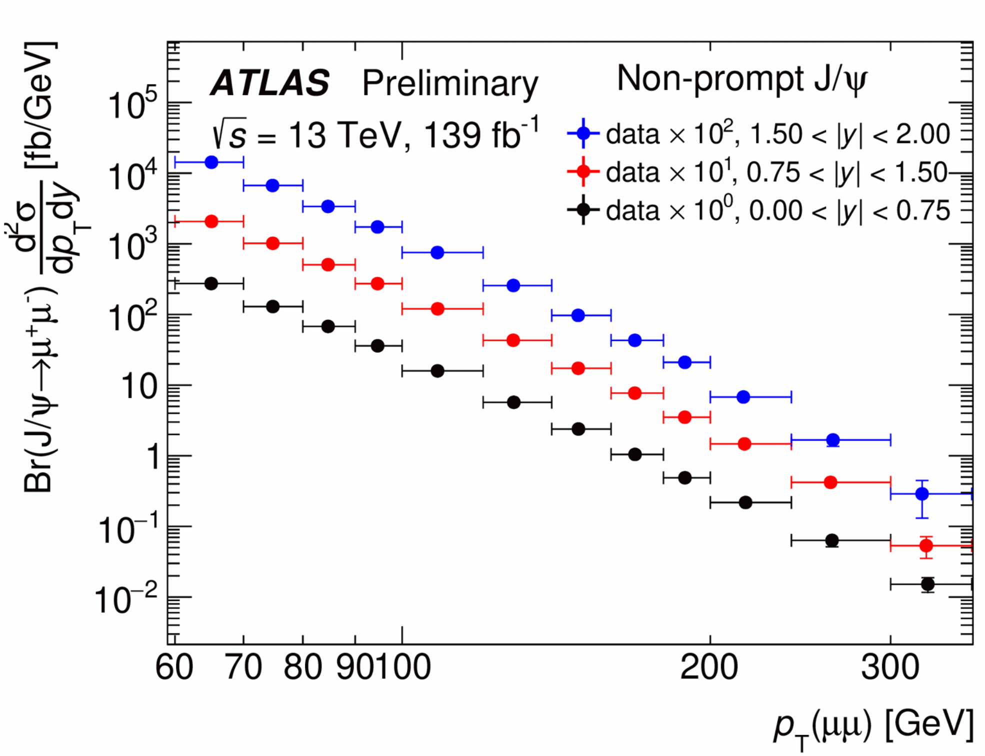

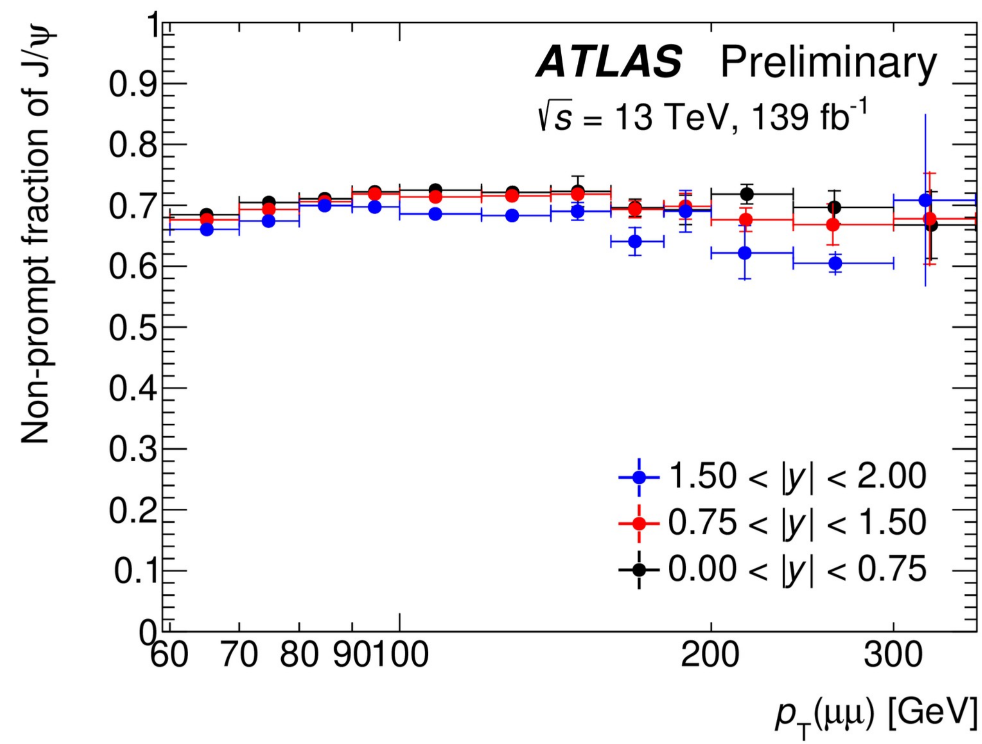

A scaling factor of 1, 10, 100 is applied for visual clarity to the rapidity slices |y|<0.75, 0.75<|y|<1.5, 1.5<|y|<2.0, respectively

Production cross section of J/ψ and ψ(2S)

ATLAS-CONF-2019-047

- Example results:
  - Predictions at FONLL for non-prompt production are consistent with measurement at the low end of p_T, but exceed the data at high p_T.

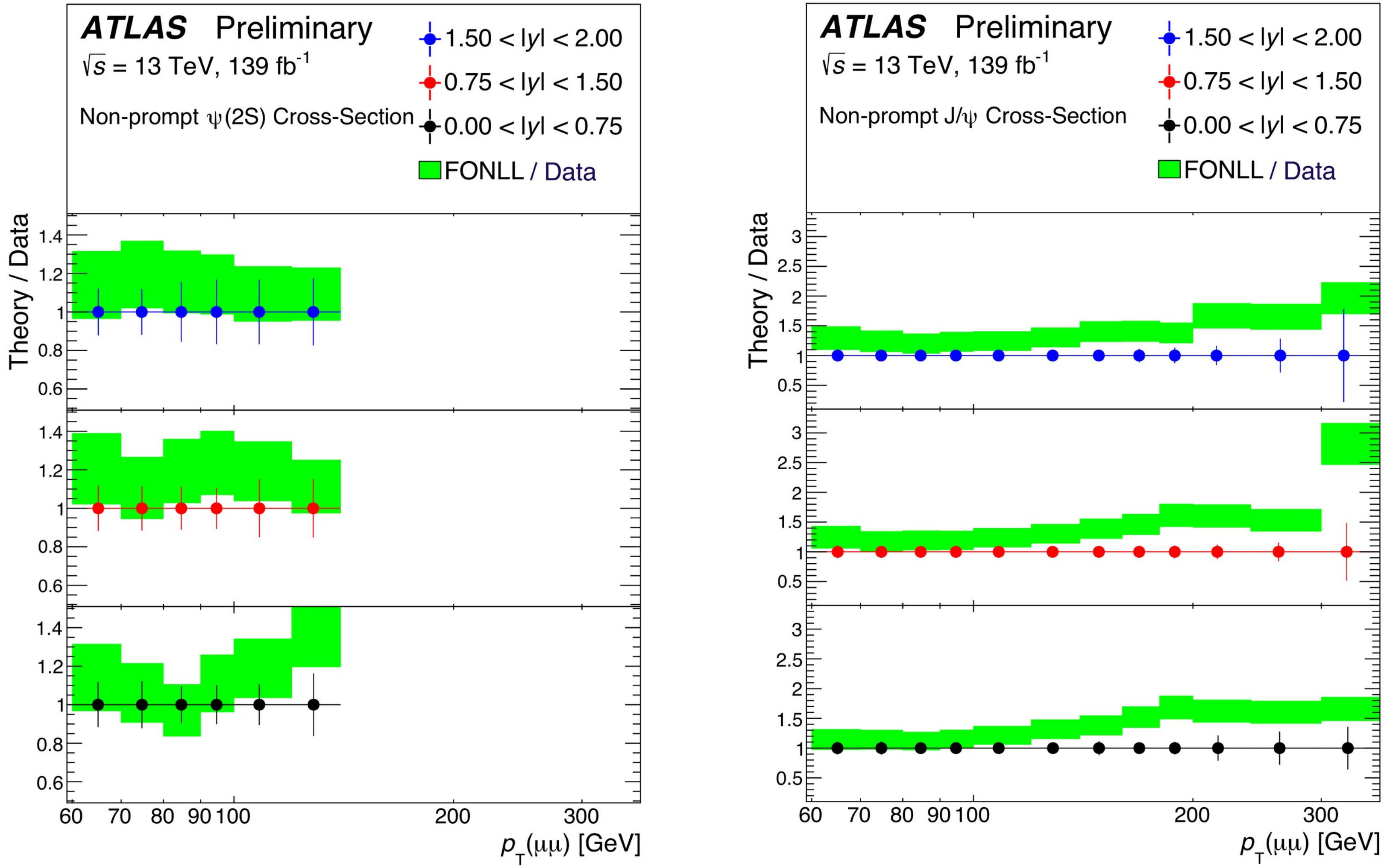

ATLAS-CONF-2019-047

Production cross section of J/ψ and ψ(2S)

- Excellent agreement between this ATLAS result for prompt J/ψ in the central rapidity range, and the CMS measurement in the closest-matching rapidity range.
  - Both sets of data are fitted to $\sim(b+p_T)^{-n}$ for b = 4.40 ± 2.33 and n = 5.91 ± 0.27,

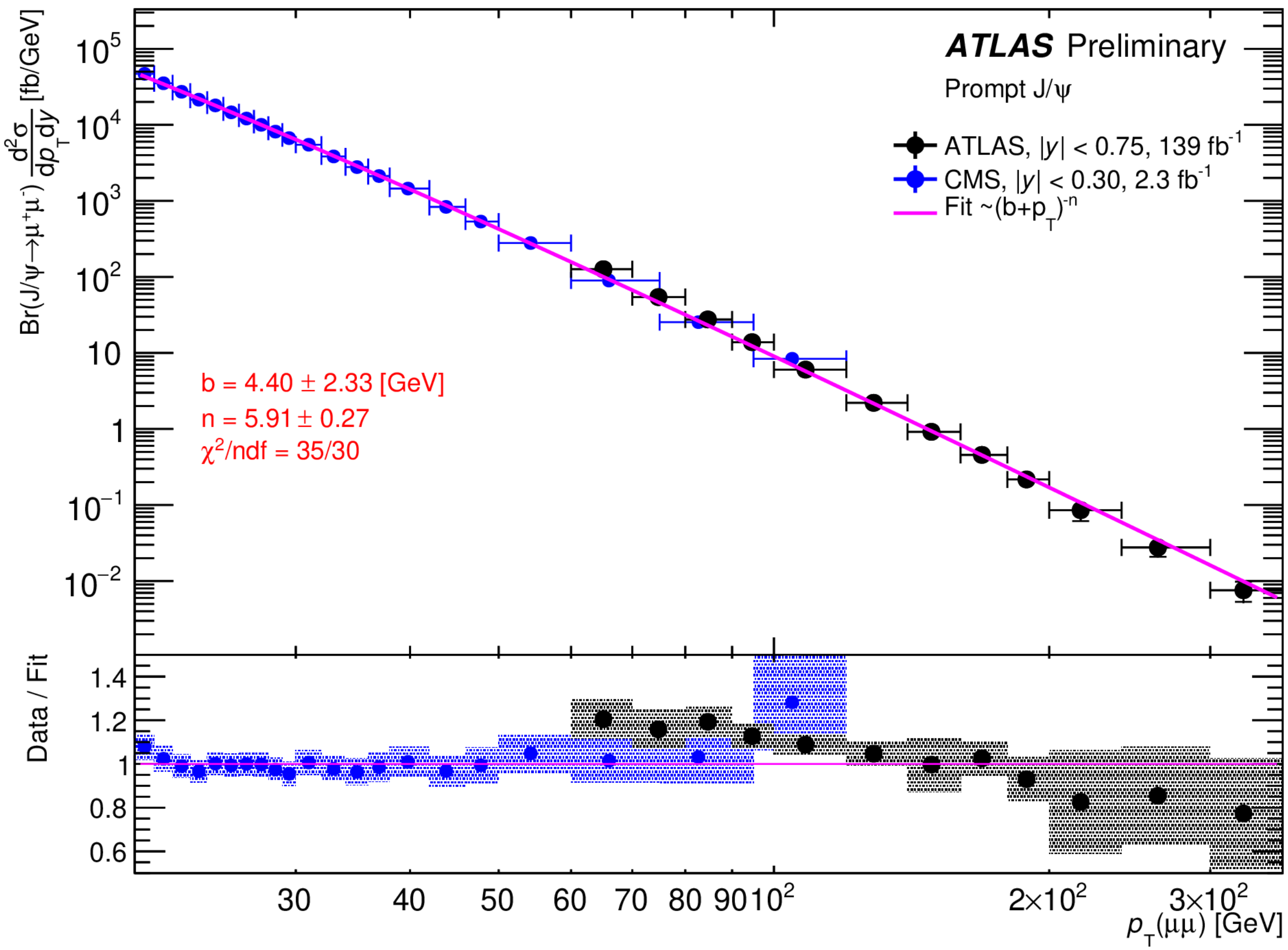

Study of $B_c^+ \rightarrow J/\psi D_s^{(*)}$ decays

Run-2 result:

arXiv:2203.01808, CERN-EP-2022-025

Study of $B_c^+ \to J/\psi D_s^{(*)}$ decays

arXiv:2203.01808
CERN-EP-2022-025

- Observed earlier by LHCb (PRD 87 (2013) 112012) and ATLAS (EPJC 76 (2016) 1) in Run 1.
- Using entire Run 2 dataset: aiming at more precise measurement of branching fractions and the final state polarisation
  - Testing predictions of various theory models, e.g. pQCD calculation, relativistic potential models, sum rules calculations..

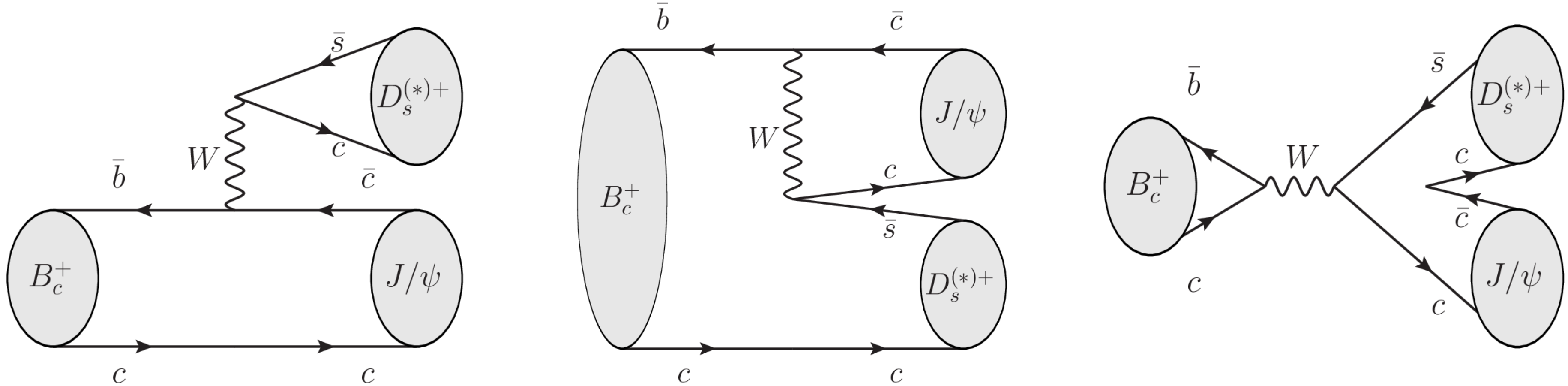

- The $B_c^+ \to J/\psi D_s^{*+}$ decay → pseudoscalar into two vector states, hence described in terms of three helicity amplitudes: A_{++}, A_{00} and A_{--},
  - the indices correspond to the helicities of the J/ψ and D_s^{*+} mesons
  - A_{++} and A_{--} amplitudes are the $A_{\pm\pm}$ component and correspond to the J/ψ and D_s^{*+} transverse polarization.
  - The fraction, $\Gamma_{\pm\pm}/\Gamma$ is also measured.

Study of $B_c^+ \to J/\psi D_s^{(*)}$ decays

arXiv:2203.01808
CERN-EP-2022-025

- D_s^+ and D_s^{*+} are reconstructed from their decays:
  - $D_s^+ \to \varphi(K^+K^-)\pi^+$
  - $D_s^{*+} \to D_s^+\ \pi^0/\gamma$ (soft, not reco)
- Use $B_c^+ \to J/\psi\pi^+$ reference channel for BR measurement
- Fiducial range: $p_T\ (B_c^+) > 15$ GeV, $|\eta(B_c^+)| < 2.0$

Reference channel with signal statistics
$N(B^+ \to J/\psi\pi^+) = 8440\ ^{+550}_{-470}$

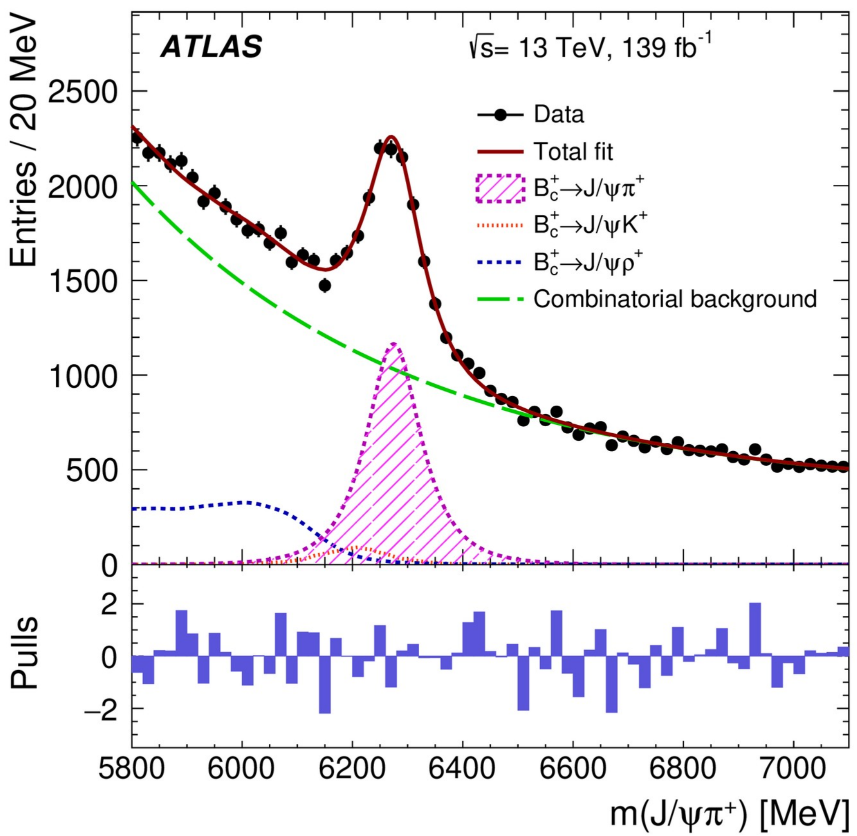

- 2D fit to extract the signal parameters
  - $m(J/\psi D_s^+)$ and the J/ψ helicity angle
- Both sensitive to polarisation of the final state particles J/ψ and D_s^+ in $B_c^+ \to J/\psi D_s^{*+}$ decay.

Study of $B_c^+ \rightarrow J/\psi D_s^{(*)}$ decays

arXiv:2203.01808
CERN-EP-2022-025

- Total yields
  - N ($B_c^+ \rightarrow J/\psi D_s^+$) = 241 ± 28 (stat)
  - N ($B_c^+ \rightarrow J/\psi D_s^{*+}$) = 424 ± 46 (stat)

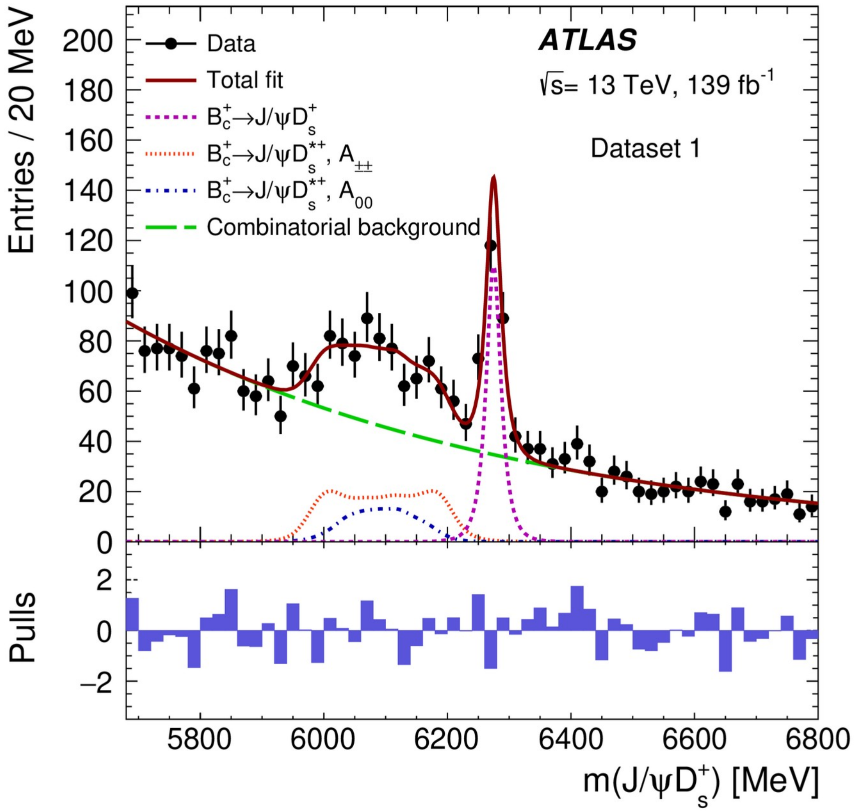

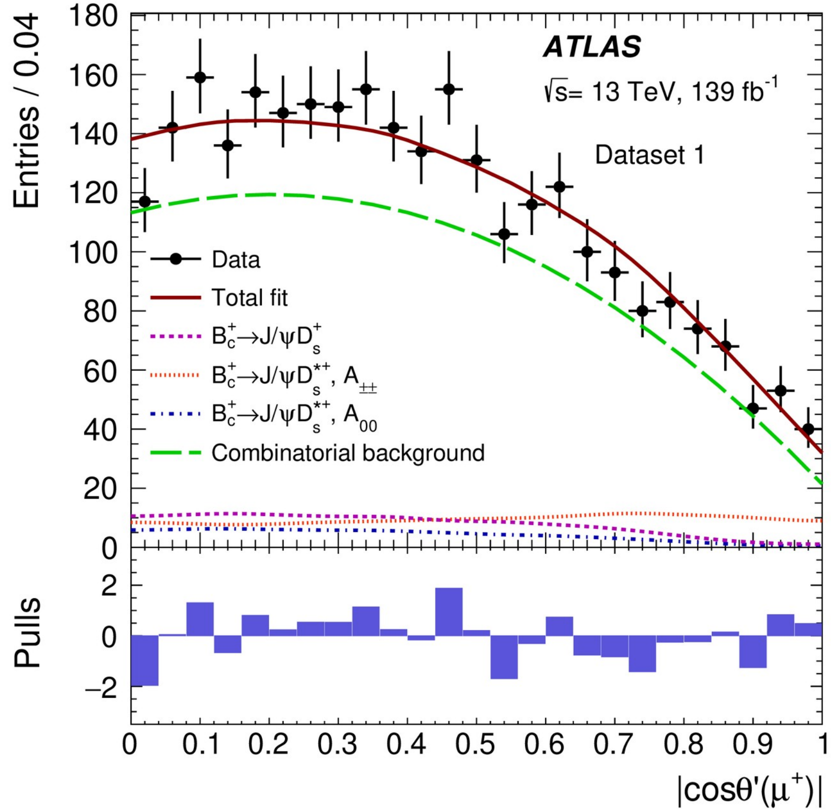

Left: fit to inv. mass $m(J/\psi D_s^+)$. Right: fit to $|\cos\theta'(\mu^+)|$, where $\theta'(\mu^+)$ is the helicity angle between μ^+ and D_s^+ momenta, in J/ψ rest frame.

Study of $B_c^+ \to J/\psi D_s^{(*)}$ decays

arXiv:2203.01808
CERN-EP-2022-025

- Results on the ratios of branching fractions and on the fraction of transverse polarization of the $B_c^+ \to J/\psi D_s^*$ decay:

Uncertainties:
(Stat) (syst) (BF)

$$R_{D_s^+/\pi^+} \equiv \mathcal{B}(B_c^+ \to J/\psi D_s^+)/\mathcal{B}(B_c^+ \to J/\psi \pi^+) = 2.76 \pm 0.33 \pm 0.30 \pm 0.16$$

$$R_{D_s^{*+}/\pi^+} \equiv \mathcal{B}(B_c^+ \to J/\psi D_s^{*+})/\mathcal{B}(B_c^+ \to J/\psi \pi^+) = 5.33 \pm 0.61 \pm 0.67 \pm 0.32$$

$$R_{D_s^{*+}/D_s^+} \equiv \mathcal{B}(B_c^+ \to J/\psi D_s^{*+})/\mathcal{B}(B_c^+ \to J/\psi D_s^+) = 1.93 \pm 0.24 \pm 0.10$$

$$\Gamma_{\pm\pm}/\Gamma(B_c^+ \to J/\psi D_s^{*+}) = 0.70 \pm 0.10 \pm 0.04$$

Study of $B_c^+ \rightarrow J/\psi D_s^{(*)}$ decays

arXiv:2203.01808
CERN-EP-2022-025

- New results consistent with earlier measurements
- $R(D_s^{*+}/\pi^+)$ described well by the predictions

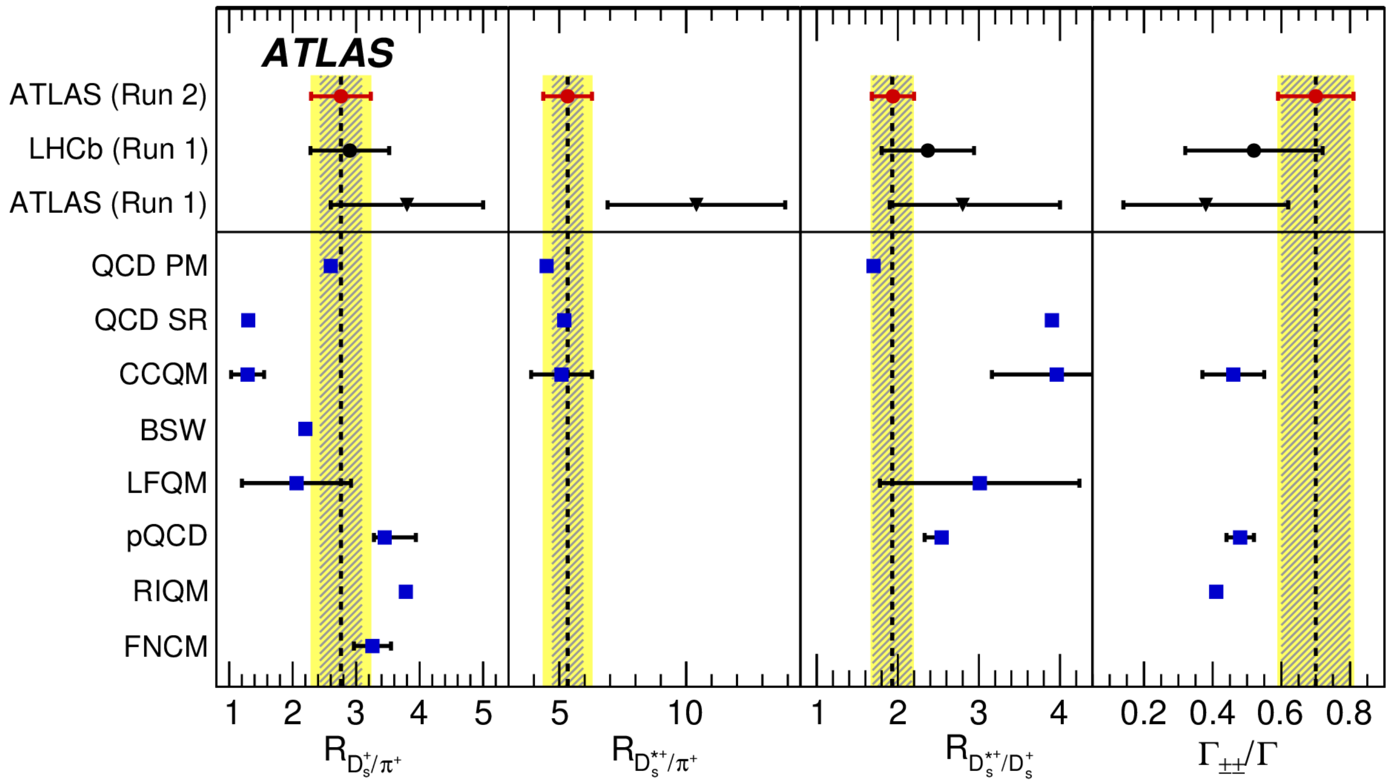

- $R(D_s^+/\pi^+)$ and $R(D_s^{*+}/D_s^+)$ predictions consistently deviate from data
  - except QCD PM (PRD 61 (2000) 034012)
- $\Gamma_{\pm\pm}/\Gamma$ agrees with a naive spin-counting estimate of 2/3 and larger than predictions
- Hatched areas → stat uncertainties; yellow bands → total uncertainties.

Conclusions

- ATLAS is competitive in B physics and b-quark studies
  - Thanks to accumulated statistical samples
  - Thanks to some detector performance (tracking)

  - **Stay tuned for on-going work towards more Run-2 analyses, while preparing for Run 3** back-up slides

arXiv:2203.01808
CERN-EP-2022-025

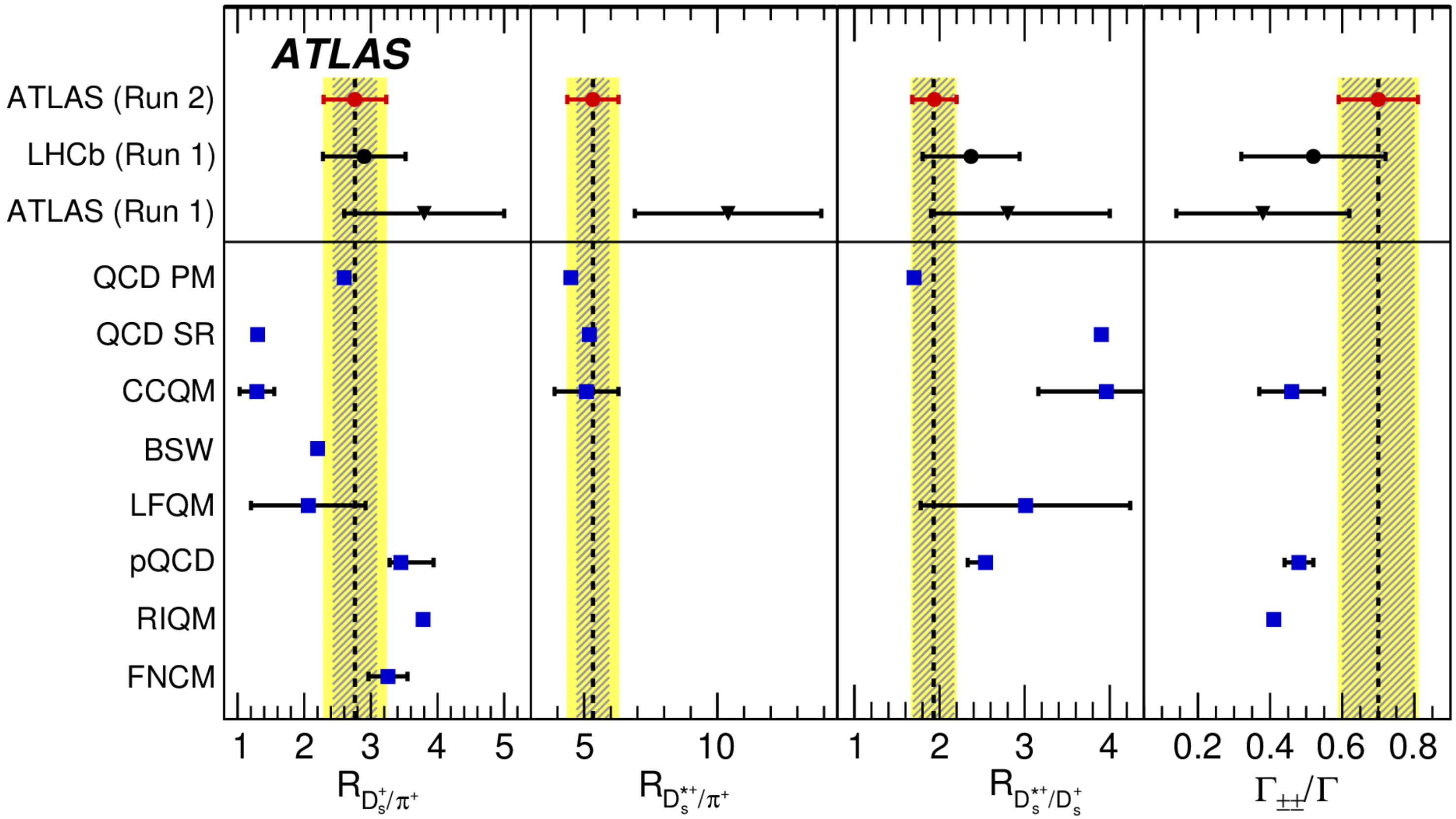

QCD PM: QCD relativistic potential model [arXiv:hep-ph/9909423, Phys. Rev. D 61, 034012 (2000)]
QCD SR: QCD sum rules [arXiv:hep-ph/0211021]
CCQM: covariant confined quark mode [arXiv:1708.09607 [hep-ph], Phys. Rev. D 96, 076017 (2017)]
BSW: Bauer-Stech-Wirbel relativistic quark model [arXiv:0810.4284 [hep-ph], Phys. Rev. D 79, 034004 (2009)]
LFQM: light-front quark mode [arXiv:1307.5925 [hep-ph], Phys. Rev. D 89, 017501 (2014)]
pQCD: perturbative QCD [arXiv:1407.5550 [hep-ph], Phys. Rev. D 90, 114030 (2014)]
RIQM: relativistic independent quark model [Phys. Rev. D 88, 094014 (2013) / arXiv:2202.01167 [hep-ph]]
FNCM: calculations in the QCD factorization approach [Int. J. Mod. Phys. A 33, 1850044 (2018), erratum 1892003]

arXiv:2203.01808
CERN-EP-2022-025

Parameter	Value
$m_{B_c^+}$ [MeV]	6274.5 ± 1.5
$\sigma_{B_c^+}$ [MeV]	47.5 ± 2.5
$N_{B_c^+ \to J/\psi\pi^+}$	8440^{+550}_{-470}

Parameter	Value
$m_{B_c^+}$ [MeV]	6274.8 ± 1.4
$\sigma_{B_c^+}$ [MeV]	11.5 ± 1.5
$r_{D_s^{*+}/D_s^+}$	1.76 ± 0.22
$f_{\pm\pm}$	0.70 ± 0.10
$N^{\mathrm{DS1}}_{B_c^+ \to J/\psi D_s^+}$	193 ± 20
$N^{\mathrm{DS2}}_{B_c^+ \to J/\psi D_s^+}$	49 ± 10
$N^{\mathrm{DS1}}_{B_c^+ \to J/\psi D_s^{*+}}$	338 ± 32
$N^{\mathrm{DS1\&2}}_{B_c^+ \to J/\psi D_s^+}$	241 ± 28
$N^{\mathrm{DS1\&2}}_{B_c^+ \to J/\psi D_s^{*+}}$	424 ± 46

arXiv:2108.11650
JHEP 12 (2021) 131

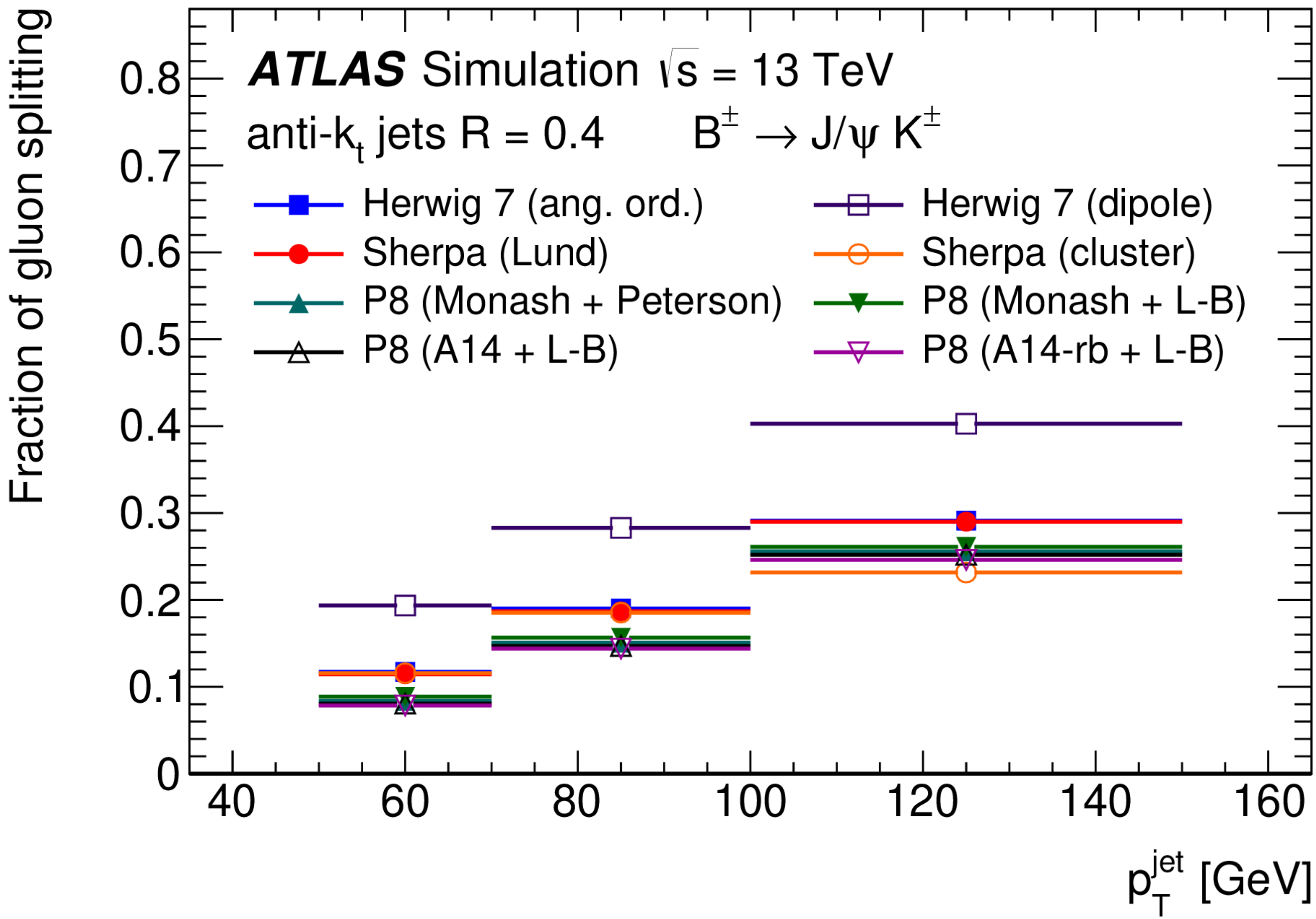

Abstract:

Recent results from the proton-proton collision data taken by the ATLAS experiment on the charmonium and B meson production and decays will be presented. The measurement of J/ψ and ψ(2S) differential cross sections will be reported as measured on the whole Run 2 dataset. The measurement of the differential cross sections of B+ production at 13 TeV and their ratios to those measured at 7 TeV will be discussed. The measurement of the differential ratios of B_c^+ and B^+ production cross sections at 8 TeV will be shown. New results on the B_c decays to J/ψ $D_s^{(*)}$ final states obtained with the Run 2 data at 13 TeV will also be reported